ENVIRONMENTAL RESEARCH
LETTERS

OPEN ACCESS

RECEIVED
30 October 2021

REVISED
9 December 2021

ACCEPTED FOR PUBLICATION
11 January 2022

PUBLISHED
26 January 2022

LETTER

Stronger Arctic amplification from ozone-depleting substances than from carbon dioxide

Yu-Chiao Liang[1,2,*], Lorenzo M Polvani[1,3,4], Michael Previdi[1], Karen L Smith[5], Mark R England[6] and Gabriel Chiodo[7]

1 Lamont-Doherty Earth Observatory, Columbia University, Palisades, NY, United States of America
2 Department of Atmospheric Sciences, National Taiwan University, Taipei, Taiwan
3 Department of Earth and Environmental Sciences, Columbia University, New York, NY, United States of America
4 Department of Applied Physics and Applied Mathematics, Columbia University, New York, NY, United States of America
5 Department of Physical and Environmental Sciences, University of Toronto, Scarborough, Toronto, Ontario, Canada
6 University of California, Santa Cruz, CA, United States of America
7 Institute for Atmospheric and Climate Science, Swiss Federal Institute of Technology Zürich, Zürich, Switzerland
* Author to whom any correspondence should be addressed.

E-mail: yuchiaoliang@ntu.edu.tw

Keywords: ozone depleting substance, carbon dioxide, Arctic amplification

Supplementary material for this article is available online

Abstract

Arctic amplification (AA)—the greater warming of the Arctic near-surface temperature relative to its global mean value—is a prominent feature of the climate response to increasing greenhouse gases. Recent work has revealed the importance of ozone-depleting substances (ODS) in contributing to Arctic warming and sea-ice loss. Here, using ensembles of climate model integrations, we expand on that work and directly contrast Arctic warming from ODS to that from carbon dioxide (CO_2), over the 1955–2005 period when ODS loading peaked. We find that the Arctic warming and sea-ice loss from ODS are slightly more than half (52%–59%) those from CO_2. We further show that the strength of AA for ODS is 1.44 times larger than that for CO_2, and that this mainly stems from more positive Planck, albedo, lapse-rate, and cloud feedbacks. Our results suggest that AA would be considerably stronger than presently observed had the Montreal Protocol not been signed.

1. Introduction

Arctic amplification (AA)—the enhanced surface warming of the Arctic compared to the global mean—is a prominent feature of climate change. It has been detected in observations in recent decades, and is robustly simulated by global climate models (Holland and Bitz 2003, Serreze *et al* 2009, Hartmann *et al* 2013). Within the Arctic, AA has resulted in substantial impacts on a wide spectrum of natural and human systems (Meredith *et al* 2019). Outside the Arctic, AA has been claimed to affect the frequency of extreme weather events in midlatitudes by altering the large-scale atmospheric circulation e.g., Francis and Vavrus (2012), Cohen *et al* (2014), Coumou *et al* (2018) although these claims and their underlying mechanisms are hotly debated e.g., Barnes (2013), Kretschmer *et al* (2016), Blackport and Screen (2020), Cohen *et al* (2020), Liang *et al* (2021). Understanding the causes of AA is, thus, not only an important scientific endeavour, but also one with regional and possibly global implications (Meredith *et al* 2019).

Much attention has been devoted to exploring the mechanisms behind AA. Many studies have emphasized the role of local feedback processes e.g., Goosse *et al* (2018), Stuecker *et al* (2018), Beer *et al* (2020), Feldl *et al* (2020), Chung *et al* (2021), of heat and moisture transport from lower latitudes e.g., Hwang *et al* (2011), Graversen and Burtu (2016), Gong *et al* (2017), Yang and Magnusdottir (2017), Yoshimori *et al* (2017), Graversen and Langen (2019), or even of biological processes e.g., Swann *et al* (2010), Park *et al* (2015, 2020), Pefanis *et al* (2020). However, much uncertainty remains as to the relative contributions from the many proposed mechanisms (Previdi *et al* 2021).

Less attention, however, has been devoted to assessing which anthropogenic forcings might be responsible for AA. There is little doubt that well-mixed greenhouse gases (GHGs) are the most important anthropogenic driver of Arctic warming e.g., Najafi *et al* (2015), Stjern *et al* (2019). While it is often assumed that the vast majority of the Arctic warming comes from CO_2, a recent study (Polvani *et al* 2020) has reported that Arctic warming would have been reduced by a factor of two if the atmospheric amount of ozone-depleting substances (hereafter, ODS, which are halogen-containing gases such as chlorofluorocarbons) had not increased between 1955 and 2005 (ODS emissions actually increased from around the mid-1950s through the 1980s, and declined rapidly thereafter). Since the radiative forcing from ODS during 1955–2005 is estimated to be about one third of the radiative forcing from CO_2 Meinshausen *et al* (2011), as estimated by, the study of Polvani *et al* (2020) raises the possibility that ODS may be more efficient at warming the Arctic than CO_2. This importance of ODS for Arctic warming has also informed in a modeling study of Goyal *et al* (2019). Using the so-called 'world avoided' scenario, they found that present-day Arctic temperatures would be 1 to 2 K warmer than observed had ODS emissions not been regulated by the Montreal Protocol.

Hence, the goal of this paper: to determine whether the AA caused by ODS is greater than the one caused by CO_2. Stjern *et al* Stjern *et al* (2019) recently quantified the AA caused by different drivers of climate change (CO_2, CH_4, black carbon, SO_4, and the solar constant), and concluded that the annual mean AA is similar among those drivers. However, ODS were not included in their study, being considered minor forcing agents. ODS have long been known to be potent greenhouse gases (Ramanathan *et al* 1987, Shine 1991), with Global Warming Potentials thousands of times larger than CO_2 Hodnebrog *et al* (2013, 2020), and have been shown to considerably affect the climate system not only at high Southern latitudes (Solomon *et al* 2015) and in the tropics (Polvani and Bellomo 2019), but also in the Arctic(Polvani *et al* 2020).

The novelty of this study, which builds on the findings of Polvani *et al* (2020), is that we here conduct and analyze new ensembles of global climate model integrations specifically designed to contrast ODS to carbon dioxide, so as to isolate and compare their respective contributions to Arctic warming over the 1955–2005 period. We not only focus on Arctic near-surface air temperature and sea-ice changes, but also show that ODS cause an AA that is 44% stronger than that caused by CO_2. We further show that ODS and CO_2 impacts are additive, and that the impact of stratospheric ozone depletion is negligible. Finally, we perform a feedback analysis to understand the underlying mechanisms that allow ODS to produce stronger AA than CO_2.

2. Methods

In this study, we examine five ensembles of simulations—each consisting of ten ensemble members differing only in their initial conditions—carried out with the Community Earth System Model Hurrell *et al* (2013), CESM, version 1: two new ensembles performed to enable explicit comparison of ODS and CO_2 impacts and three ensembles from Polvani *et al* (2020). The simulations cover the 1955–2005 period, when ODS forcing increased rapidly Polvani *et al* (2020), see figure 1 in . The first ensemble consists of ten historical integrations performed by the CESM Large Ensemble Project (Kay *et al* 2015), hereafter referred to as *ALL*, to indicate that these runs were forced by all natural and anthropogenic historical forcings following the Coupled Model Intercomparison Project Phase 5 protocol Taylor *et al* (2012). The second and third ensembles of integrations, conducted as part of the Polvani *et al* (2020) study, are identical to *ALL* except that in the second ensemble the ODS concentrations are fixed at 1955 levels, while in the third ensemble both ODS and stratospheric ozone concentrations are fixed at their 1955 levels. To cleanly isolate the effect of CO_2, we performed a fourth ensemble of integrations with CO_2 concentrations fixed at 1955 levels. And finally, to test the linear additivity of the response to CO_2 and ODS, we performed a fifth ensemble of integrations with both CO_2 and ODS concentrations fixed at their 1955 levels.

Focusing on the differences between the *ALL* ensemble and the fixed-forcing ensembles allows us to isolate the effect of the individual forcings on the Arctic climate. This leave-one-out approach follows Polvani *et al* (2011) and many others, including the recent studies contrasting the effects of aerosols and GHGs in the CESM Large Ensemble (Deng *et al* 2020, Deser *et al* 2020, England 2021). In the following analyses, we refer to the difference between the *ALL* and the fixed-ODS ensembles as ODS, as it isolates the impacts of ODS. Similarly CO_2 stands for the difference between the *ALL* and fixed-CO_2 ensembles, as it isolates the impacts of CO_2. Again, CO_2 and ODS indicates the difference between the *ALL* and fixed-CO_2-and-ODS ensembles. Finally, the impacts of stratospheric ozone are quantified as the difference between the fixed-ODS and fixed-ODS-and-O_3 ensembles, and is denoted as *Strat-*O_3.

To investigate the physical processes producing AA, we perform a feedback analysis based on the top-of-atmosphere (TOA) energy budget over the Arctic domain,

$$\Delta R + \Delta F - \Delta H = 0, \quad (1)$$

where ΔR denotes the change in net downward radiation at the TOA, ΔF the change in horizontal convergence of atmospheric and oceanic energy transports, and ΔH the change in the ocean heat storage (derived from ocean potential temperatures) in the Arctic, assuming that ocean uptake dominates and contributions from the atmosphere, land, and cryosphere are negligible due to their relatively small heat capacities. We estimate ΔF as the difference between ΔH and ΔR (with the latter calculated from model output TOA radiative fluxes). ΔR can be decomposed as follows:

$$\Delta R = \Delta R_F + \Delta R_{Planck} + \Delta R_{LR} + \Delta R_{AL} + \Delta R_{WV} + \Delta R_{CL}, \quad (2)$$

where ΔR_F denotes the stratosphere-adjusted radiative forcing calculated with the Parallel Offline Radiative Transfer (PORT) model assuming fixed dynamical heating (Conley *et al* 2013), ΔR_{Planck} the Planck feedback due to vertically uniform warming, ΔR_{LR} the lapse-rate feedback due to vertically non-uniform warming, ΔR_{AL} the surface albedo feedback, ΔR_{WV} the water vapor feedback, and ΔR_{CL} the cloud feedback (calculated using the adjusted cloud radiative effect method of Soden *et al* (2008)). For the Planck feedback, we show the deviation from the global-mean value, and we refer to this as Planck'. The residual (or error) in our decomposition of ΔR is estimated as the difference between ΔR calculated directly from model output TOA radiative fluxes, and ΔR calculated from equation (2). We use the Community Atmosphere Model version 5 radiative kernels (Pendergrass *et al* 2018) to compute the feedbacks in equation (2).

We focus on the annual and Arctic-mean energy budget differences between two 10-year time periods, 1996–2005 and 1955–1964; this methods yields results that are very similar to the those obtained from linear trend analysis (discussed in Polvani *et al* (2020)). We divide each component of equation (2) by the change in Arctic-mean surface air temperature (ΔT_s) to derive feedback parameters.

To test the statistical significance of trend differences, we perform a two-sided Student's *t*-test with the null hypothesis that the difference of 10-member ensemble-mean trends is zero. If the null hypothesis can be rejected with 10% significance level (i.e. the *p*-value less than 0.10), we refer to the ensemble-mean trends as statistically different or separable. To test the robustness of our results and minimize the effect of internal variability, we employ a bootstrapping technique (Pedregosa *et al* 2011) and randomly sample twenty members from each ensemble of integrations 10 000 times with replacement (results are not sensitive to how many members are selected). We average over each of the re-sampled members to obtain distributions of 10 000 ensemble means.

We also look at ΔT_s from the observational large-ensemble dataset provided by McKinnon and Deser (2018). This dataset informs us about the effects of internal variability, and also allows us to determine whether our model simulations are in line with observations.

In the analysis that follows, Arctic-mean values refer to the area-weighted average for the variable of interest over the Arctic domain, i.e. 60°N–90°N. Similarly, global-mean (tropical-mean) values denote the area-weighted average over the global (tropical) domain, i.e. 90°S–90°N (30°S–30°N).

3. Results

We begin by comparing the forced annual-mean Arctic warming and September sea-ice loss in *ODS* to those in *ALL* and *CO2* via examining the spatial distributions of their ensemble-mean surface air temperature (SAT) and sea-ice concentration (SIC) trends (figure 1). The SAT trends in ALL are comparable to those in CO_2, but with greater warming in the Laptev-East Siberian Seas, Barents-Kara Seas, and East Greenland Sea (c.f., figures 1(a) and b). Correspondingly, large negative September SIC trends appear in these regions in *ALL* and *CO2* (c.f., figures 1(e) and f). In contrast, *ODS* shows the strongest warming trends in the Laptev-East Siberian Seas, accompanied by large sea-ice loss in that region (figures 1(c) and g).

To quantitatively compare the 1955–2005 *CO2* and *ODS* trends over the Arctic, we plot the Arctic-mean annual-mean SAT trends for the ensemble averages, and for the individual ensemble members, in box-and-whisker plots in figure 2(a). Let us start by comparing the *ALL* and *CO2* ensembles. The ensemble-mean SAT trend in *ALL* is 0.32 $K \cdot decade^{-1}$, which is only slightly larger than the ensemble-mean trend for *CO2*, of 0.27 $K \cdot decade^{-1}$. Note the considerable overlap between the *ALL* and *CO2* SAT trend distributions derived from 10 000 re-samples from bootstrapping (c.f., black and magenta distributions in figure 2(b). In fact, the *ALL* trends are statistically inseparable from the *CO2* ones. Keeping in mind that the *CO2* trends do not include the effect of aerosol forcings which is, however, present in the *ALL* trends, we conclude that—in this model, over the Arctic—the aerosol forcing is greatly offset by the presence of the other (non-CO_2) greenhouse gases. This is also seen in the September sea-ice extent (SIE) trends, which are only slightly larger in *ALL* than in *CO2*, but with no statistically significant difference (figure 2(c)). For completeness, the entire seasonal evolution of the Arctic-mean SAT and SIE trends is shown in figure S1 (available online at stacks.iop.org/ERL/17/024010/mmedia): it shows

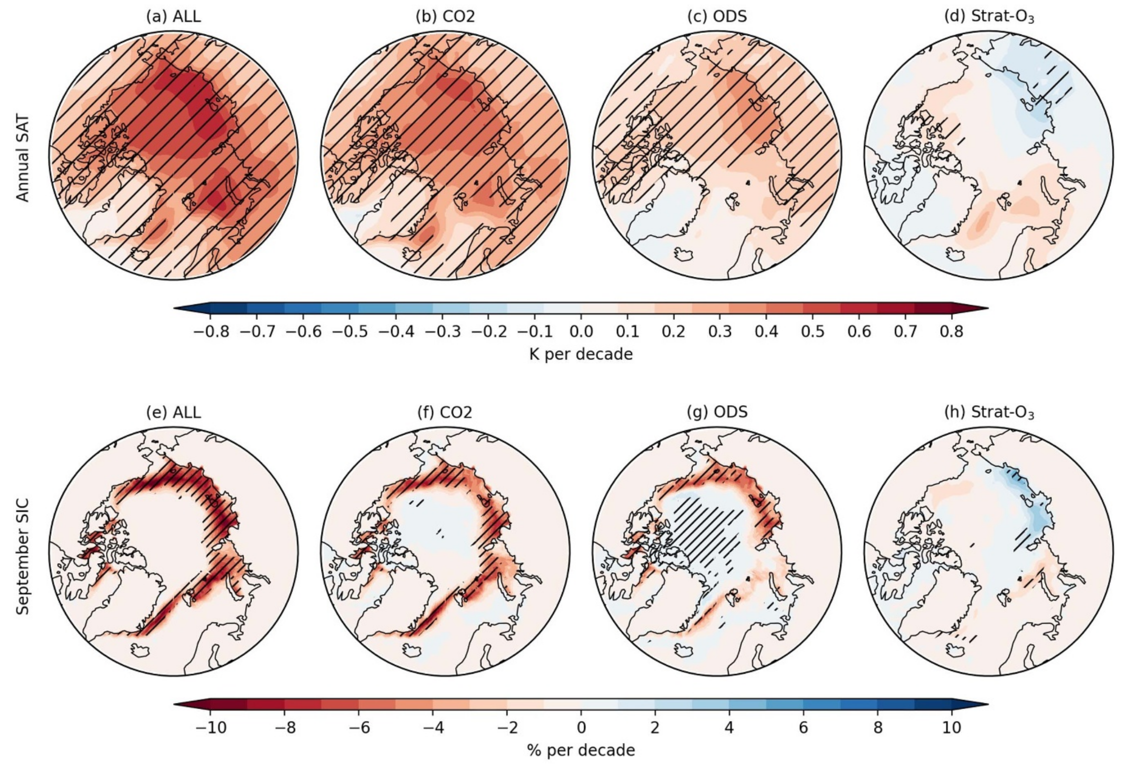

Figure 1. Spatial distributions of annual-mean 1955–2005 SAT trends for (a) *ALL*, (b) *CO2*, (c) *ODS*, and (d) *Strat-O_3*. (e)–(h): as in (a)–(d), but for September SIC trends. Hatched regions indicate where trends are significant at the 5% significance level using a Student's *t*-test. The trend shown here is first calculated for each member in *ALL* and fixed-forcing runs separately, then taking their difference, and finally averaging over ensemble members.

strong warming trends during late autumn and substantial Arctic sea-ice loss trends from August to October for both ensembles.

Let us now turn our attention to ODS, which contributed the largest non-CO_2 increase in radiative forcing over the period 1955–2005 Myhre *et al* (2013), see, for instance, the orange bars in figure 8.6d of. As one can see in figure 2, the *ODS* ensemble-mean Arctic SAT trend is 0.14 $K \cdot decade^{-1}$, which is slightly more than half (52 ± 35%, uncertainty is estimated by the full range of maximum and minimum difference between *ODS* and *CO2*) the *CO2* ensemble-mean value. This difference in Arctic SAT trend is statistically significant at 10% level. A similarly large response to ODS is found for sea ice: the September SIE ensemble-mean trend for *ODS* is $-0.16 \times 10^6 \cdot km^2 \cdot decade^{-1}$, which again is more than half of the *CO2* ensemble-mean value of $-0.27 \times 10^6 \cdot km^2 \cdot decade^{-1}$. This is an unexpected result, as the radiative forcing of ODS over this period is only one third of the CO_2 forcing Polvani *et al* (2020), see figure 1 in: the radiative forcing of ODS accounts for 28% of the CO_2 forcing over the Arctic domain based on our PORT model simulations, slightly larger than the estimate from Polvani *et al* (2020). Such discrepancy could be further understood if the effective radiative forcings of ODS and CO_2 are estimated. Clearly some enhanced climate feedbacks must at work under ODS forcing.

Before examining those, however, we ask whether the response to CO_2 and ODS, the two largest well-mixed greenhouse-gas forcings over the half-century 1955–2005, is linearly additive. The question is answered in figure 2(a) (c.f., brown and green clusters). In our 10-member ensembles, we see no statistically significant difference between the *CO2&ODS* trends, in which *both* CO_2 and ODS increase in the model integrations over that period, and the sum of the *CO2* and *ODS* trends (denoted *CO2+ODS*), in which CO_2 and ODS alone increase in the model simulations, respectively. This linear additivity result holds for both annual-mean SAT and September SIE (and annual SIE shown in figure S2).

Since the increase of ODS is accompanied by the destruction of ozone, we also explore the potential impact of stratospheric ozone depletion over the Arctic. Much work has been done on the climate impacts of ozone depletion: while capable of reaching into the subtropics e.g., Kang *et al* (2011) those impacts have been largely confined to the Southern Hemisphere Previdi and Polvani (2014), for a comprehensive review, see, although a few studies have suggested a possible impact on the Northern Hemispheric circulation (Smith and Polvani 2014, Calvo *et al* 2015). Over the Arctic, however, our model simulations (see the *Strat-O_3* results in figures 1 and 2) show that the impact of stratospheric ozone on SAT and SIE is negligible (with trends of 0.02 $K \cdot decade^{-1}$ and

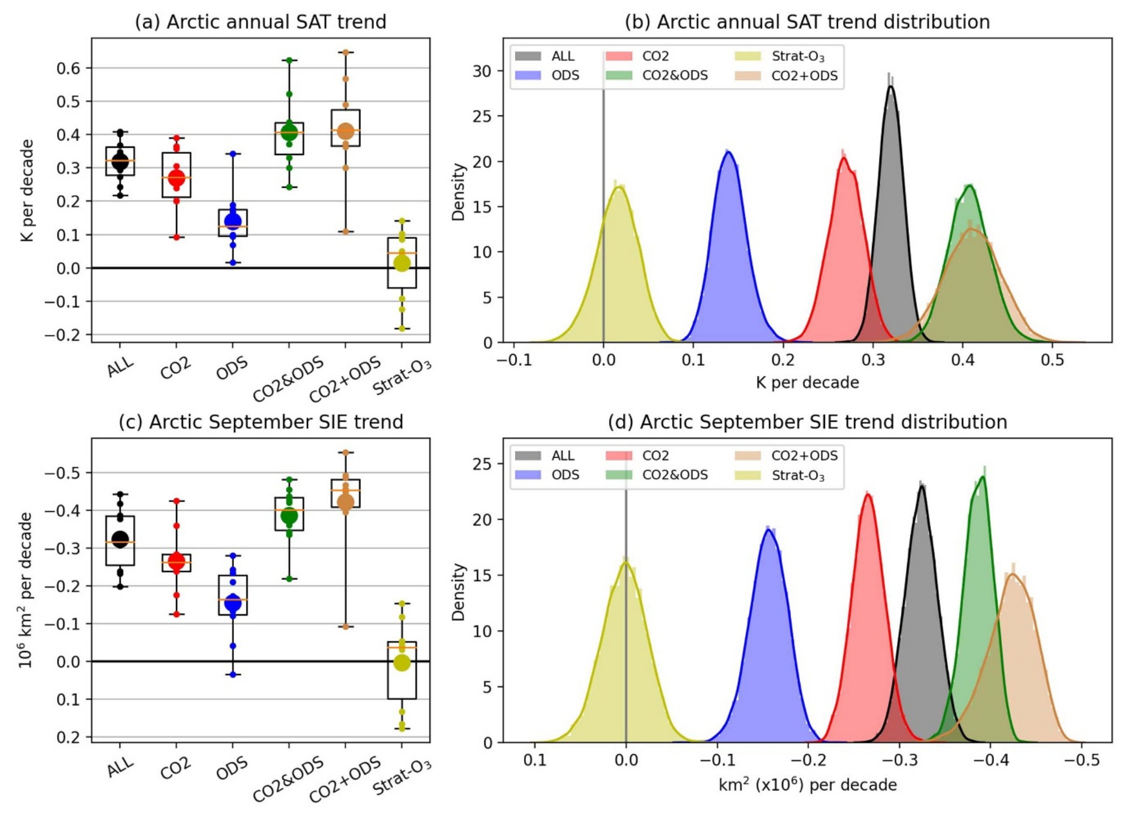

Figure 2. (a) Arctic-mean annual SAT trends for *ALL*, *CO2*, *ODS*, *CO2&ODS*, *CO2+ODS* (sum of *CO2* and *ODS*), and *Strat-O*$_3$. The large dots show the ensemble-mean values, and the small dots the individual members. The whiskers show the ranges of 10-member ensembles, and the orange horizontal lines their median values. (b) Probability density functions for 10 000 re-sampled annual Arctic-mean SAT trends for *ALL*, *CO2*, *ODS*, *CO2&ODS*, *CO2+ODS* (sum of *CO2* and *ODS*), and *Strat-O*$_3$. (c) and (d): as in (a) and (b), but for Arctic September SIE trends.

-0.002×10^6 km$^2 \cdot$ decade^{-1}, respectively, which are not significantly different from zero). This should not be surprising, as the radiative forcing from ozone depletion is small even over Antarctica (Chiodo *et al* 2017), where stratospheric ozone loss is much larger than over the Arctic.

Let us now turn to AA, and specifically to contrasting AA caused by ODS to AA caused by CO_2, which is the main goal of this study. We start by examining the Arctic-mean SAT trends against global-mean trends for *ODS* and *CO2* (figure 3(a)). First, note that the SAT trends for *CO2* are larger than for *ODS*, for both Arctic and global means; this is expected because the radiative forcing from CO_2 is larger than the one from ODS during the 1955–2005 time period Polvani *et al* (2020), see figure 1 in. The ensemble-mean global SAT trend for *CO2* (big red dot in figure 3(a) is 2.67 times larger than that for *ODS* (big blue dot in figure 3(a). However, for Arctic SAT trends the former is only 1.92 times larger than the letter, suggesting a weaker Arctic warming forced by CO_2 than by ODS with respect to global warming—a manifestation of AA signature. Second, AA occurs in both *CO2* and *ODS*, and is clearly visible from the fact that the ensemble means (large red and blue dots) are found above the one-to-one line (in dashed gray) that marks where Arctic and global warming trends are of equal magnitude. Third, we estimate the strength of AA from the linear least-squares slope of Arctic SAT trends against global SAT trends using the 10 000 re-sampled ensembles. We find that the *ODS* slope (3.59 $\pm$ 0.05, solid blue line) is significantly larger than the *CO2* slope (2.73 $\pm$ 0.06, solid red line), indicating that ODS causes a stronger AA than CO_2.

To facilitate the quantitative comparison of AA in the *ODS* and *CO2* ensembles, we define the AA factor (AAF) as the ratio of the Arctic-mean SAT trend to the global-mean SAT trend. These AAFs for each *ODS* and *CO2* member, and for their ensemble-mean values, are graphically illustrated with box-and-whisker plots in figure 3(b). Consistent with the regression analysis in figure 3(a), the *ODS* ensemble-mean AAF (3.82) is larger than the *CO2* ensemble-mean AAF (2.64) by a factor of 1.44. They are also statistically separable. We also show identical diagnostics for *ALL* (black lines, dots, and cluster in figures 3(a) and b): these are similar to those of *CO2*, as expected. In addition, the AAF for the ensemble-mean of observational large ensemble (2.62, green dots) is similar to those for *ALL* and *CO2*, suggesting the modeled AAFs are in line with the observational estimate. The above results clearly indicate that AA from ODS is larger than AA from CO_2, and suggest that ODS are more effective GHGs than CO_2 in terms of generating AA.

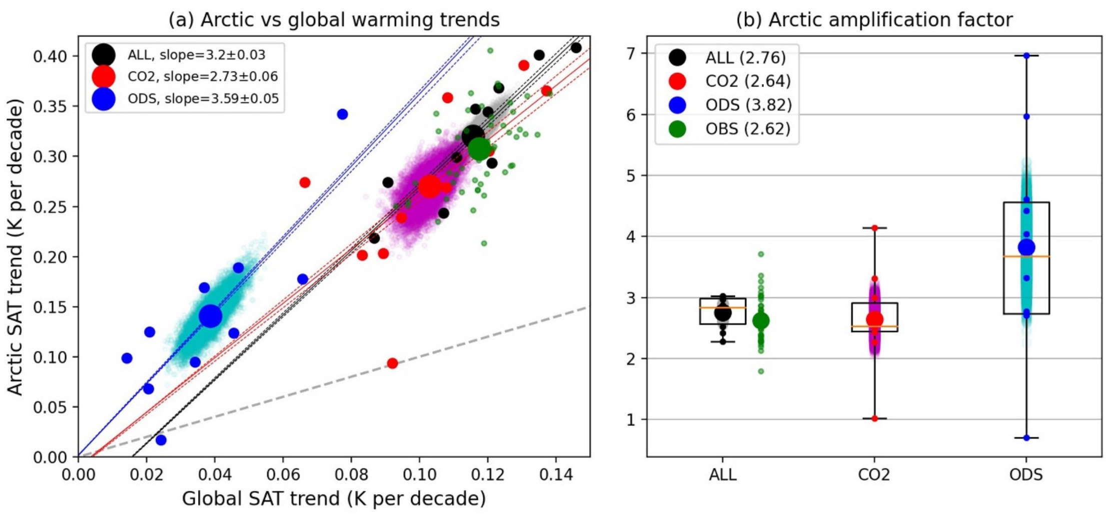

Figure 3. (a) The Arctic-mean annual SAT trends vs. the global-mean annual SAT trends, for *ODS* (blue cluster), *CO2* (red cluster), and *ALL* (black cluster). The big dots show the ensemble-mean values, and the small dots the individual members. The solid and dashed lines are the linear least-squares fits and the corresponding 95% confidence interval range from the 10 000 re-samples. The dashed gray line has one-to-one slope. (b) Box-and-whisker plots for the Arctic amplification factor (AAF), with the whiskers showing the ranges of 10-member ensembles, and the orange horizontal lines showing the median values for *ALL*, *CO2*, and *ODS*. The big dots are the ensemble-mean values, the smaller dots the individual members. In both panels, the gray, magenta and cyan lighter dots show the 10 000 re-samples. The green dots present the results obtained from observational large ensemble.

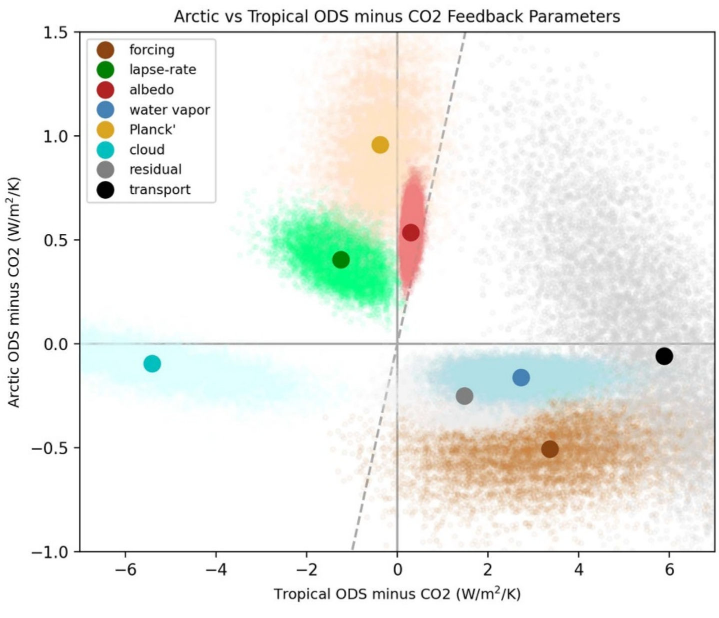

Figure 4. The *ODS* minus *CO2* Arctic vs. tropical annual feedback parameters for Planck' (golden), lapse-rate (green), surface albedo (dark red), water vapor (dark blue), net cloud (longwave plus shortwave, cyan), and convergence of atmospheric and oceanic heat transports (black), as well as forcing (dark brown) and residual (gray). The big dots denote the ensemble-mean values and the dots with light colors the values of 10 000 re-samples. The dashed gray line has one-to-one slope.

Finally, we elucidate the mechanisms leading to a stronger AA in *ODS* than in *CO2*. In *ODS* and *CO2* individually, AA can be explained by more positive Planck', surface albedo, lapse-rate, and cloud feedbacks over the Arctic compared to the tropics (figures S3a and S3b). We find that differences in these same feedbacks between *ODS* and *CO2* (figure 4) explains the stronger AA from ODS than from CO_2 forcing. In contrast, differences in radiative forcing, water vapor feedback, and energy transport response act to oppose the stronger AA in *ODS* (as evidenced by the fact that these terms lie below the one-to-one line in figure 4). It is worth noting that the *ODS* and *CO2* cloud feedback parameters are nearly identical in the Arctic, but the former is more negative than the latter in the tropics. We are currently investigating the reasons for these feedback differences between *ODS* and *CO2*—including the seasonality of those differences and of AA—and we plan to report on this in a future paper.

4. Summary and discussion

Building on the recent study of Polvani *et al* (2020), who highlighted the importance of ODS in warming the Arctic during the second half of the 20th century (when ODS became regulated by the Montreal Protocol), we have here further explored how ODS compare to CO_2 in terms of their Arctic impact with new large-ensemble simulations conducted. Using ensembles of global climate model integrations designed to isolate the respective impacts of ODS and CO_2 over the period 1955–2005, we have found that the Arctic warming and September sea-ice melting from ODS are slightly more than half of their CO_2 counterparts. This, we have shown, is due to the fact that AA caused by ODS is larger than the one caused by CO_2 (the AAF for ODS is 1.44 times larger than for CO_2). And, finally, we have determined that differences in Planck', surface albedo, lapse-rate, and cloud feedbacks between *ODS* and *CO2* can explain the stronger AA in response to ODS forcing. It will be important to validate these results with different climate models, and with larger ensembles, although Arctic climate responses consistent with ours have been reported in a recent study using a different climate model (Goyal *et al* 2019).

In conclusion, it is important to appreciate that while the large global warming potential of ODS has been known since the mid-seventies (Ramanathan 1975), it is only in the last decade that we have started to appreciate the profound and broad climate impacts of these gases. Well beyond causing the ozone hole over Antarctica, it is now clear that ODS have substantially contributed to global warming and to Arctic sea-ice loss. These recent findings confirm that the Montreal Protocol, originally signed to protect the stratospheric ozone layer, is in reality a major climate mitigation treaty as ODS affect the entire planet. The continued monitoring of ODS, therefore, is not only beneficial for the ozone hole healing in the Southern Hemisphere, but also a matter of great importance for Arctic climate change.

Data availability statement

The data that support the findings of this study are available upon reasonable request from the authors.

Acknowledgments

This work is supported by grants from the National Science Foundation to Columbia University (award numbers 1603350 and 1914569). G C acknowledges support by the Swiss Ambizione grant PZ00P2_180043. Y C L is also supported by the grant of the Ministry of Science and Technology (MOST 110-2111-M-002-019-MY2) to National Taiwan University. The computing and data storage resources, including the Cheyenne supercomputer (doi:10.5065/D6RX99HX), were provided by the Computational and Information Systems Laboratory at National Center for Atmospheric Research (NCAR). NCAR is a major facility sponsored by the U.S. NSF under Cooperative Agreement 1852977. The CESM large-ensemble model output (i.e. *ALL*) can be obtained from NCAR (www.cesm.ucar.edu/projects/community-projects/LENS/data-sets.html), while variables of other ensembles of integrations are processing and will be available on the Arctic Data Centre archive of the NSF Office of Polar Programs (https://arcticdata.io/).

ORCID iDs

Yu-Chiao Liang https://orcid.org/0000-0002-9347-2466
Lorenzo M Polvani https://orcid.org/0000-0003-4775-8110
Michael Previdi https://orcid.org/0000-0001-7701-1849
Karen L Smith https://orcid.org/0000-0002-4652-6310
Mark R England https://orcid.org/0000-0003-3882-872X
Gabriel Chiodo https://orcid.org/0000-0002-8079-6314

References

Barnes E A 2013 Revisiting the evidence linking Arctic amplification to extreme weather in midlatitudes *Geophys. Res. Lett.* **40** 4734–9

Beer E, Eisenman I and Wagner T J 2020 Polar amplification due to enhanced heat flux across the halocline *Geophys. Res. Lett.* **47** e2019GL086706

Blackport R and Screen J A 2020 Weakened evidence for mid-latitude impacts of Arctic warming *Nat. Clim. Change* **10** 1–2

Calvo N, Polvani L M and Solomon S 2015 On the surface impact of Arctic stratospheric ozone extremes *Environ. Res. Lett.* **10** 094003

Chiodo G, Polvani L and Previdi M 2017 Large increase in incident shortwave radiation due to the ozone hole offset by high climatological albedo over Antarctica *J. Clim.* **30** 4883–90

Chung E-S, Ha K-J, Timmermann A, Stuecker M F, Bodai T and Lee S-K 2021 Cold-season arctic amplification driven by arctic ocean-mediated seasonal energy transfer *Earth's Future* **9** e2020EF001898

Cohen J *et al* 2014 Recent Arctic amplification and extreme mid-latitude weather *Nat. Geosci.* **7** 627–37

Cohen J *et al* 2020 Divergent consensuses on Arctic amplification influence on midlatitude severe winter weather *Nat. Clim. Change* **10** 20–9

Conley A, Lamarque J-F, Vitt F, Collins W and Kiehl J 2013 PORT, a CESM tool for the diagnosis of radiative forcing *Geosci. Model Dev.* **6** 469–76

Coumou D, Di Capua G, Vavrus S, Wang L and Wang S 2018 The influence of Arctic amplification on mid-latitude summer circulation *Nat. Commun.* **9** 1–12

Deng J, Dai A and Xu H 2020 Nonlinear climate responses to increasing CO_2 and anthropogenic aerosols simulated by CESM1 *J. Clim.* **33** 281–301
Deser C, Phillips A S, Simpson I R, Rosenbloom N, Coleman D, Lehner F, Pendergrass A G, DiNezio P and Stevenson S 2020 Isolating the evolving contributions of anthropogenic aerosols and greenhouse gases: a new CESM1 large ensemble community resource *J. Clim.* **33** 7835–58
England M R 2021 Are multi-decadal fluctuations in arctic and antarctic surface temperatures a forced response to anthropogenic emissions or part of internal climate variability? *Geophys. Res. Lett.* **48** e2020GL090631
Feldl N, Po-Chedley S, Singh H K, Hay S and Kushner P J 2020 Sea ice and atmospheric circulation shape the high-latitude lapse rate feedback *npj Clim. Atmos. Sci.* **3** 1–9
Francis J A and Vavrus S J 2012 Evidence linking Arctic amplification to extreme weather in mid-latitudes *Geophys. Res. Lett.* **39** L06801
Gong T, Feldstein S and Lee S 2017 The role of downward infrared radiation in the recent arctic winter warming trend *J. Clim.* **30** 4937–49
Goosse H *et al* 2018 Quantifying climate feedbacks in polar regions *Nat. Commun.* **9** 1–13
Goyal R, England M H, Gupta A S and Jucker M 2019 Reduction in surface climate change achieved by the 1987 Montreal Protocol *Environ. Res. Lett.* **14** 124041
Graversen R G and Burtu M 2016 Arctic amplification enhanced by latent energy transport of atmospheric planetary waves *Q. J. R. Meteorol. Soc.* **142** 2046–54
Graversen R G and Langen P L 2019 On the Role of the Atmospheric Energy Transport in 2× CO_2–induced polar amplification in CESM1 *J. Clim.* **32** 3941–56
Hartmann D L *et al* 2013 Observations: atmosphere and surface *Climate Change 2013 the Physical Science Basis: Working Group I Contribution to the Fifth Assessment Report of the Intergovernmental Panel on Climate Change* (Cambridge: Cambridge University Press) pp 159–254
Hodnebrog Ø, Aamaas B, Fuglestvedt J, Marston G, Myhre G, Nielsen C, Sandstad M, Shine K P and Wallington T 2020 Updated global warming potentials and radiative efficiencies of halocarbons and other weak atmospheric absorbers *Rev. Geophys.* **58** e2019RG000691
Hodnebrog Ø, Etminan M, Fuglestvedt J, Marston G, Myhre G, Nielsen C, Shine K P and Wallington T 2013 Global warming potentials and radiative efficiencies of halocarbons and related compounds: a comprehensive review *Rev. Geophys.* **51** 300–78
Holland M M and Bitz C M 2003 Polar amplification of climate change in coupled models *Clim. Dyn.* **21** 221–32
Hurrell J W *et al* 2013 The community earth system model: a framework for collaborative research *Bull. Am. Meteorol. Soc.* **94** 1339–60
Hwang Y-T, Frierson D M and Kay J E 2011 Coupling between Arctic feedbacks and changes in poleward energy transport *Geophys. Res. Lett.* **38** L17704
Kang S M, Polvani L, Fyfe J and Sigmond M 2011 Impact of polar ozone depletion on subtropical precipitation *Science* **332** 951–4
Kay J E *et al* 2015 The community earth system model (CESM) large ensemble project: a community resource for studying climate change in the presence of internal climate variability *Bull. Am. Meteorol. Soc.* **96** 1333–49
Kretschmer M, Coumou D, Donges J F and Runge J 2016 Using causal effect networks to analyze different Arctic drivers of midlatitude winter circulation *J. Clim.* **29** 4069–81
Liang Y-C *et al* 2021 Impacts of Arctic sea ice on cold season atmospheric variability and trends estimated from observations and a multimodel large ensemble *J. Clim.* **34** 8419–43
McKinnon K A and Deser C 2018 Internal variability and regional climate trends in an observational large ensemble *J. Clim.* **31** 6783–802
Meinshausen M *et al* 2011 The RCP greenhouse gas concentrations and their extensions from 1765 to 2300 *Clim. Change* **109** 213–41
Meredith M *et al* 2019 Chapter 3: Polar regions *IPCC Special Report on the Ocean and Cryosphere in a Changing Climate*
Myhre G *et al* 2013 Anthropogenic and natural radiative forcing Climate change 2013: The Physical Science Basis *Contribution of Working Group I to the Fifth Assessment Report of the Intergovernmental Panel on Climate Change* 659–740
Najafi M R, Zwiers F W and Gillett N P 2015 Attribution of Arctic temperature change to greenhouse-gas and aerosol influences *Nat. Clim. Change* **5** 246–9
Park J-Y, Kug J-S, Bader J, Rolph R and Kwon M 2015 Amplified Arctic warming by phytoplankton under greenhouse warming *Proc. Natl Acad. Sci.* **112** 5921–6
Park S-W, Kim J-S and Kug J-S 2020 The intensification of Arctic warming as a result of CO_2 physiological forcing *Nat. Commun.* **11** 1–7
Pedregosa F *et al* 2011 Scikit-learn: machine learning in python *J. Mach. Learn. Res.* **12** 2825–30 (available at: https://jmlr.org/papers/v12/pedregosa11a.html)
Pefanis V, Losa S N, Losch M, Janout M A and Bracher A 2020 Amplified arctic surface warming and sea ice loss due to phytoplankton and colored dissolved material *Geophys. Res. Lett.* **47** e2020GL088795
Pendergrass A G, Conley A and Vitt F M 2018 Surface and top-of-atmosphere radiative feedback kernels for CESM-CAM5 *Earth Syst. Sci. Data* **10** 317–24
Polvani L M and Bellomo K 2019 The key role of ozone-depleting substances in weakening the walker circulation in the second half of the twentieth century *J. Clim.* **32** 1411–18
Polvani L M, Previdi M, England M R, Chiodo G and Smith K L 2020 Substantial twentieth-century Arctic warming caused by ozone-depleting substances *Nat. Clim. Change* **10** 130–3
Polvani L M, Waugh D W, Correa G J and Son S-W 2011 Stratospheric ozone depletion: the main driver of twentieth-century atmospheric circulation changes in the Southern Hemisphere *J. Clim.* **24** 795–812
Previdi M and Polvani L M 2014 Climate system response to stratospheric ozone depletion and recovery *Q. J. R. Meteorol. Soc.* **140** 2401–19
Previdi M, Smith K L and Polvani L M 2021 Arctic amplification of climate change: a review of underlying mechanisms *Environ. Res. Lett.* **16** 093003
Ramanathan V 1975 Greenhouse effect due to chlorofluorocarbons: climatic implications *Science* **190** 50–2
Ramanathan V *et al* 1987 Climate-chemical interactions and effects of changing atmospheric trace gases *Rev. Geophys.* **25** 1441–82
Serreze M, Barrett A, Stroeve J, Kindig D and Holland M 2009 The emergence of surface-based Arctic amplification *Cryosphere* **3** 11–19
Shine K P 1991 On the cause of the relative greenhouse strength of gases such as the halocarbons *J. Atmos. Sci.* **48** 1513–18
Smith K L and Polvani L M 2014 The surface impacts of Arctic stratospheric ozone anomalies *Environ. Res. Lett.* **9** 074015
Soden B J, Held I M, Colman R, Shell K M, Kiehl J T and Shields C A 2008 Quantifying climate feedbacks using radiative kernels *J. Clim.* **21** 3504–20
Solomon A, Polvani L M, Smith K and Abernathey R 2015 The impact of ozone depleting substances on the circulation, temperature and salinity of the Southern Ocean: an attribution study with CESM1 (WACCM) *Geophys. Res. Lett.* **42** 5547–55
Stjern C W *et al* 2019 Arctic amplification response to individual climate drivers *J. Geophys. Res.: Atmos.* **124** 6698–6717
Stuecker M F *et al* 2018 Polar amplification dominated by local forcing and feedbacks *Nat. Clim. Change* **8** 1076–81

Swann A L, Fung I Y, Levis S, Bonan G B and Doney S C 2010 Changes in Arctic vegetation amplify high-latitude warming through the greenhouse effect *Proc. of the National Academy of Sciences* vol 107 pp 1295–300

Taylor K E, Stouffer R J and Meehl G A 2012 An overview of CMIP5 and the experiment design *Bull. Am. Meteorol. Soc.* **93** 485–98

Yang W and Magnusdottir G 2017 Springtime extreme moisture transport into the Arctic and its impact on sea ice concentration *J. Geophys. Res.: Atmos.* **122** 5316–29

Yoshimori M, Abe-Ouchi A and Laîné A 2017 The role of atmospheric heat transport and regional feedbacks in the Arctic warming at equilibrium *Clim. Dyn.* **49** 3457–72